TECHNICAL REPORT STANDARD PAGE

1. Report No.	2. Government Accession No.	3. Recipient's Catalog No.
FHWA/LA-92/253		

4. Title and Subtitle	5. Report Date
ENGINEERING PROPERTIES OF BRITTLE REPAIR MATERIALS	SEPTEMBER 1992
	6. Performing Organization Code

7. Author(s)	8. Performing Organization Report No.
G. Z. VOYIADJIS, C. CHANNAKESHAVA, T.M. ABU-LEBDEH, F. BARZEGAR	253

9. Performing Organization Name and Address	10. Work Unit No.
Department of Civil Engineering Louisiana State University Baton Rouge, LA 70803	11. Contract or Grant No. 89-2C

12. Sponsoring Agency Name and Address	13. Type of Report and Period Covered
Louisiana Transportation Research Center P.O. Box 94245, Capitol Station Baton Rouge, LA 70804-9245	Summary Report July 1989 - June 1992
	14. Sponsoring Agency Code

15. Supplementary Notes

Conducted in cooperation with the U.S. Department of Transportation, Federal Highway Administration.

16. Abstract

Most codes of practice prescribe procedures for selecting patch configuration and materials based on test devised for evaluating new pavement materials. This study is aimed at examining the special consideration to be given to such evaluation procedures and to suggest improved procedures for brittle repair materials, based on additional tests and computer analysis.

The first part of the present investigation covers the experimental study, in which three different repair materials, namely plain concrete, steel fiber concrete, and rapid patch material (Duracel cement) are investigated. Tests are conducted on two different patch configurations (transition and rectangular) and three different patch depths (2, 4 and 6 inches). The experimental procedure to evaluate a brittle repair material consider four tests, namely, uniaxial strength test, biaxial strength test, bond strength tests, and shear test of a repaired pavement joint. As a result of the experimental study, it is concluded that the proposed biaxial testing set-up has been shown to provide a better understanding by which the strength and behavior of brittle repair materials can be fully investigated. It is observed that the strength of the repair material under combined tension and compression is lower than under uniaxial compression, and the strength decreases as the applied tensile stress in increased.

In the second part of this study, a mechanistic patched pavement analysis program is developed to assist in the evaluation of patching procedures and materials. Such a program can be used to develop curves which aid in the selection process. It can also be used for a case by case analysis for specific problems. This program can analyze both intact and patched concrete pavements considering different loading and support conditions, material properties, patch configurations, and depths. In this study, for the first time a complete distress simulation capability has been built into a three dimensional analysis program and it is expected that analysis using this program would enable better understanding of pavement behavior, which can lead to proper guidelines for evaluation of different materials and repair procedures in rehabilitating rigid-jointed pavements.

The full report is presented in two volumes and is issued as report number FHWA/LA-92/254.

17. Key Words	18. Distribution Statement
concrete, bi-axial testing, concrete pavement modeling, concrete engineering properties testing	Unrestricted. This document is available to the public through the National Technical Information Service, Springfield, VA 22161.

19. Security Classif. (of this report)	20. Security Classif. (of this page)	21. No. of Pages	22. Price
Unclassified	Unclassified	55	

Form DOT F1700.7 (1-92)

ENGINEERING PROPERTIES OF BRITTLE REPAIR MATERIALS

SUMMARY REPORT

by

G. Z. VOYIADJIS
PROFESSOR OF CIVIL ENGINEERING
C. CHANNAKESHAVA
RESEARCH ASSOCIATE
T. M. ABU-LEBDEH
DOCTORAL CANDIDATE
F. BARZEGAR
ASSISTANT PROFESSOR OF CIVIL ENGINEERING
DEPARTMENT OF CIVIL ENGINEERING
LOUISIANA STATE UNIVERSITY
BATON ROUGE, LA 70803

CONDUCTED FOR

LOUISIANA DEPARTMENT OF TRANSPORTATION AND DEVELOPMENT
LOUISIANA TRANSPORTATION RESEARCH CENTER
in Cooperation with
U.S. Department of Transportation
FEDERAL HIGHWAY ADMINISTRATION

APRIL 1992

ABSTRACT

Most codes of practice prescribe procedures for selecting patch configuration and materials based on tests devised for evaluating new pavement materials. This study is aimed at examining the special considerations to be given to such evaluation procedures and to suggest improved procedures for brittle repair materials, based on additional tests and computer analysis.

The first part of the present investigation covers the experimental study, in which three different repair materials, plain concrete, steel fiber concrete, and rapid patch material (Duracal cement) are investigated. Tests are conducted on two different patch configurations (transition and rectangular) and three different patch depths (2, 4, and 6 inches). The experimental procedure to evaluate a brittle repair material consists of four tests, uniaxial strength test, biaxial strength test, bond strength test, and shear test of a repaired pavement joint. As a result of the experimental study, we conclude that the proposed biaxial testing set-up has been shown to provide a better understanding by which the strength and behavior of brittle repair materials can be fully investigated. We observed that the strength of the repair material under combined tension and compression is lower than under uniaxial compression, and the strength decreases as the applied tensile stress is increased.

In the second part of this study, a mechanistic patched pavement analysis program is developed to assist in the evaluation of patching procedures and materials. Such a program can be used to develop curves which aid in the selection process. It can also be used for a case by case analysis of specific problems. This program can analyze both intact and patched concrete pavements considering different loading and support conditions, material properties, patch configurations, and depths. In this study, for the first time, a complete distress simulation capability has been built into a three-dimensional analysis program. We expect that analysis using this program will enable better understanding of pavement behavior, which can lead to proper guidelines for evaluation of different materials and repair procedures in rehabilitating rigid-jointed pavements.

The full report is presented in two volumes and is issued as report number FHWA/LA-92/254.

ACKNOWLEDGMENTS

This work was carried out under contract with the Louisiana Transportation Research Center sponsored by the Federal Highway Administration and the Louisiana Department of Transportation and Development. The authors gratefully acknowledge the support and the encouragement of Harold Paul, William Temple, and Masood Rasoulian.

We would also like to express our appreciation for the help provided by the laboratory technicians of LTRC, Richard P. Desselles, Randy C. Young, Matt A. Tircuit, and the LTRC concrete research engineer, Nick Rabalais.

PROGRAM IMPLEMENTATION

A mechanistic patched pavement analysis program has been developed to assist in the evaluation of patching procedures and materials. The program could be used to develop curves which aid in the selection process. It could also be used for a case by case analysis for specific problems. Further, detailed information of stresses in pavement sections can be obtained from the program. The application of the program can be enhanced by minor modifications. Only the development of the curves necessary for evaluating the patch repair materials and configurations need some special knowledge which can be obtained through special training. Not much training or effort is necessary to use these curves. If guidelines for basic inputs and range of variation are supplied the authors assure assistance in developing these curves, or in training the personnel of the user departments in the use of the program.

TABLE OF CONTENTS

LIST OF TABLES

LIST OF FIGURES

Chapter 1

INTRODUCTION

Concrete pavements are commonly used for their durability and ability to sustain subgrade weakness and difficult climatic conditions. In spite of care in design and construction, many concrete pavements have not performed adequately and have displayed local failures including cracking, spalling, faulting, etc. It is not always economical to replace the whole slab. In most cases, repair works are undertaken. These constitute full and partial depth patches either with ordinary concrete or special brittle repair materials. Most codes of practice prescribe procedures for selecting patch configuration and materials based on tests devised for evaluating new pavement materials. This study is aimed at examining the special considerations to be given to such evaluation procedures and to suggest improved procedures for brittle repair materials, based on additional tests and computer analysis.

Chapter 2

MOTIVATION AND OBJECTIVES

The standard procedure to evaluate a brittle repair material consists of four tests. These are:

1. Uniaxial compression test: In this test a cylindrical specimen is subjected to a compressive load until failure and the uniaxial compressive strength is obtained.
2. Flexure test: A beam specimen is subjected to a central concentrated load until failure and modulus of rupture is computed.
3. Split shear test: In this test, a cylindrical specimen is cut along an inclined surface and the patch material is cast on this surface after coating it with a suitable bond material. This specimen is tested in uniaxial compression and the bond strength of the joint is obtained.
4. Shrinkage test: This test measures the change in length of a specimen.

All these specimens are subjected to very simple stress states in these tests. In a material insensitive to stress states, these tests are sufficient and give reasonably good estimates of the quality and suitability of the materials for use as pavement patching materials. However, concrete and most of the brittle repair materials are sensitive to stress states. Figure 1. shows the strength envelope of concrete under biaxial stress fields. In biaxial compression, concrete shows improved strength. But, in biaxial compression-tension stress fields, concrete shows a marked sensitivity to the stress ratio. If the tensile strength of concrete is 300 psi when the lateral compressive stress is zero, it may reduce to 150 psi for a lateral compressive stress of 1500 psi. Likewise, under tensile stresses, the compressive strength reduces rapidly. Codes have not considered this aspect of concrete behavior in developing test procedures. Further, for different repair materials, this behavior may vary. Since the tensile strength (or the modulus of rupture) is an important property on which most designs are based, it is important that a reasonably good estimate of this strength for the region under consideration is obtained. As repair works are undertaken in regions of distress, these are obviously regions of high stress concentrations and selection of a patch configuration and the material for repair should consider the most critical stress state that can exist in this region. For these reasons, testing of concrete and other repair materials in a state of biaxial compression-tension stress state can be considered to be a more realistic and safe material evaluation procedure. Most such tests, developed for concrete, have been performed using sophisticated testing machines and advanced testing technology. Such facilities are not available in the conventional material testing laboratory. This fact motivated the development of a

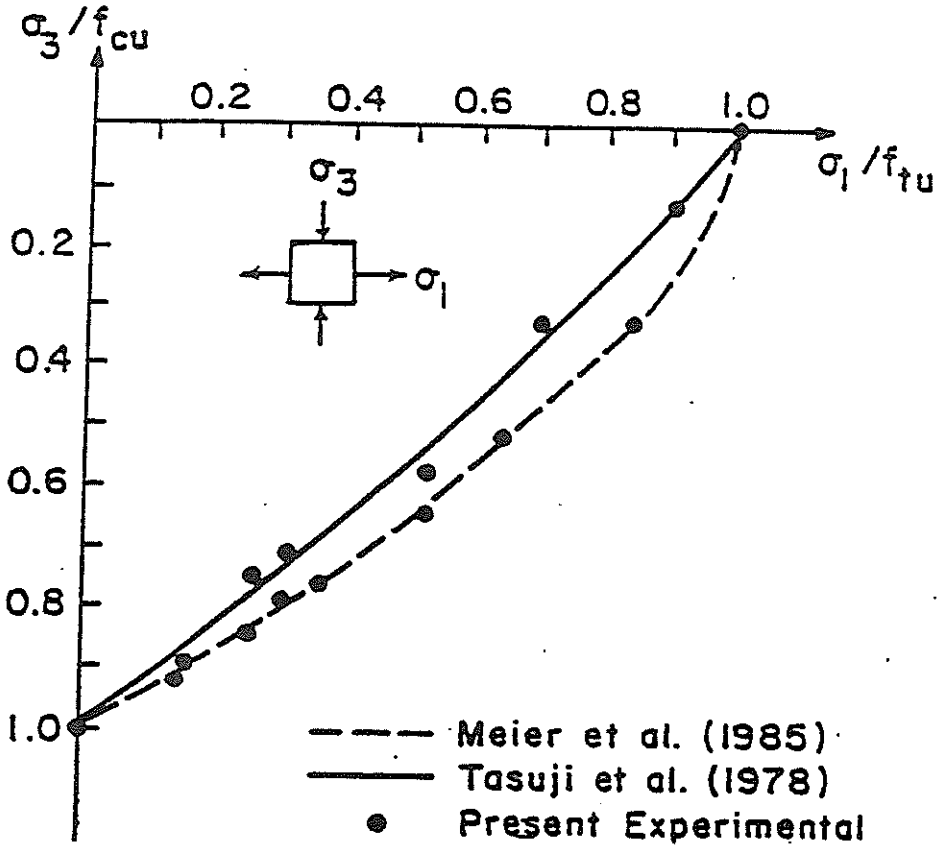

Figure 1
Ultimate strength envelope of biaxial tension-compression

simple testing procedure for testing materials under biaxial tension-compression stress states using the universal testing machine normally available in testing laboratories.

Concrete, being sensitive to the stress state, responds differently when different specimen shapes are employed. A safety factor in the design equations usually takes care of this variation. However, it would be more appropriate to develop a specimen shape which is much more representative of the field conditions than the conventional cylinders. Pavements, being flat and rectangular, can be better represented by a rectangular specimen than a cylindrical specimen.

As already described, the stress state, or in other words the ratio of the tension to compression stresses, is very important in determining the tensile strength of the material. The laboratory procedure can be used to develop the strength envelope by performing a number of tests on the same material. A number of tests with different stress ratios have to be conducted for this purpose. Since testing is an expensive procedure, it would be more advantageous if the critical stress ratio for any given pavement, patch configuration, loading, and support conditions, is identified beforehand and then the test is performed using this ratio to obtain the necessary strength information. The complexity of the stress condition in pavements has resulted in the inability of the conventional analysis procedures to yield sufficiently accurate stress values for the various wheel load positions and subgrade support conditions. To obtain this information a computer program has been developed employing the powerful finite element method of analysis. A preliminary analysis using this program can give the most critical stress ratio at any point of the pavement for different conditions of loading. This information can be used in the tests to obtain the necessary strength properties.

Understanding the effects of critical loading conditions, both wheel loads and climatic effects such as temperature, is crucial to the development of an effective repair procedure for pavements. All the major modes of distress should be simulated analytically to obtain the necessary information. The computer program developed in this study aids in this process by considering the major distresses: cracking and yielding of concrete, loss of subgrade support due to pumping, and loss of dowel support due to local yielding and cracking of concrete.

Another important property, particularly for the repair material, is the shrinkage. Normally, a material with as little shrinkage as possible should be selected. Many times economics governs selection and shrinkage of the material is unavoidable. Information regarding the effect of shrinkage of repair materials on the performance of pavements is scarce. Since shrinkage introduces tensile stresses in the repair material, it is expected that under the combined action of wheel loads, temperature stresses, and shrinkage stresses, the overall tensile stresses increase. If these stresses increase beyond the tensile strength of the repair material, cracks occur. However, this has not been observed in thefield. But, there is a secondary effect.

Even though the tensile stresses do not increase enough to cause cracking, the ratio of tensile stress to tensile strength increases and may become more than 50 percent even for smaller wheel loads. As shown in Figure 2, if the stress to strength ratio exceeds 50 percert, the number of applications of such loads reduces. Smaller wheel loads (say 9 kips equivalent single axle loads ESAL) are much more frequent than large wheel loads and hence, in terms of years, the life of pavement reduces. This load results in fatigue failure of patched sections and occurs near the junction of patched and existing pavement sections. Since laboratory experiments are expensive, a computer simulation of shrinkage effects would be more desirable. Such a simulation is also included in this study.

Thus, the present study concentrates on two aspects:

1. Development of a simple testing procedure that can be conducted in any normal testing laboratory, and which can consider the biaxial tension-compression stress states, along with the development of a simple specimen which is more representative of patched pavement sections than the conventional specimen.
2. Development of a computer program which uses some of the results of the tests and in turn assisting in further tests and which can analyze concrete pavements considering cracking and crushing of concrete, loss of subgrade support, development of temperature and shrinkage strains, etc, so as to provide more information to the designer than conventional analytical procedures.

The following sections describe briefly the two phases of the project and highlight the important conclusions and recommendations.

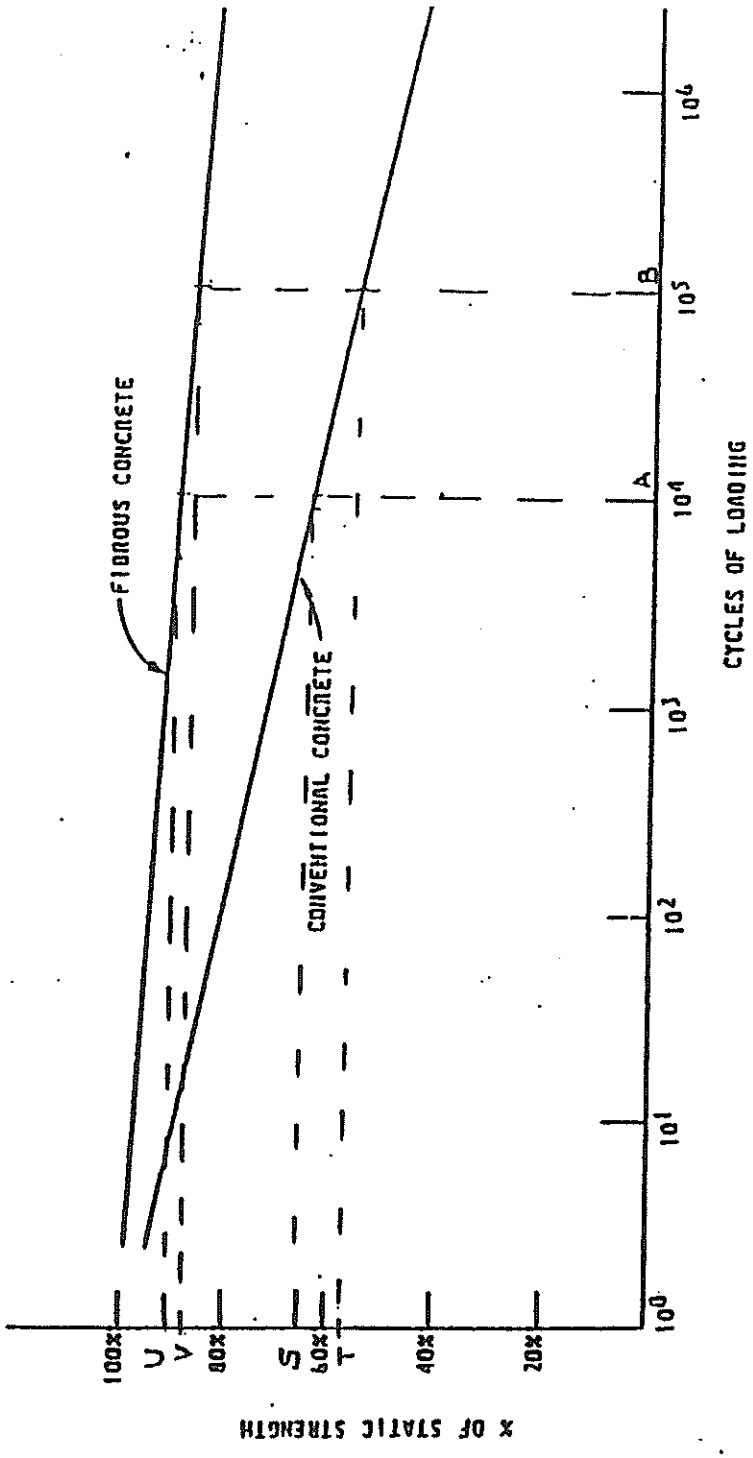

Figure 2
Typical fatigue curves for concrete and fiber concrete *[6]*

Chapter 3

EXPERIMENTAL PROGRAM

3.1 Standard Uniaxial Test Specimens

The experimental program consists of standard strength tests and biaxial loading tests on a specially designed specimen and set-up. The standard strength tests were conducted for calibration and comparisons. The tests conducted were:

1. Uniaxial compressive strength test conducted on cylindrical specimens in accordance with the ASTM standards C-39
2. Flexural tensile strength test on prismatic beam specimens in accordance with the ASTM standards C-78
3. Tests for determining the elastic properties, the Young's modulus and the Poisson's ratio, in accordance with the ASTM standards C-469.
4. Splitting tensile strength test on cylindrical specimens in accordance with ASTM standards C-496.

Concrete for the tests was prepared in accordance with the ASTM standards C-192. In all thirty-eight cylinders (6 in x 12 in) for uniaxial compression tests, thirty-four cylinders (6 in x 12 in) for splitting tensile test, and thirty-eight rectangular beams (6 in x 6 in x 20 in) for the flexural strength test were cast. Some of the cylindrical specimens were used to determine the elastic properties. These tests showed that the procedure and method employed yield results that are within the acceptable range of variation as specified in respective standards.

The test specimens were instrumented to obtain the stress-strain response of the specimens under different loading conditions. The stress-strain curves obtained compared well with available test results.

3.2 Biaxial Test Specimens

For the biaxial testing of materials, no standards are available. In order to achieve the main objective of this experimental phase, a special test set-up and specimen were developed.

Test Set-up

The test set-up developed and employed for biaxial testing of concrete is shown in Figure 3. This consists of a metal frame, to which hydraulic jacks can be attached at two sides. Provisions are made in the housing of these jacks so that adjustments to alignment can be made easily. Tension is applied by means of these jacks and through steel bars. Compression is applied by placing the testing frame in a universal testing machine.

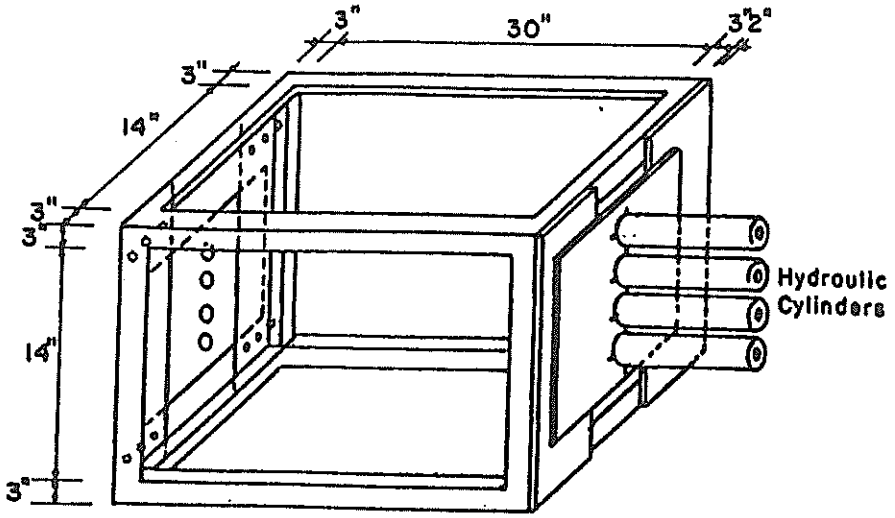

(a) Details of the biaxial test set-up

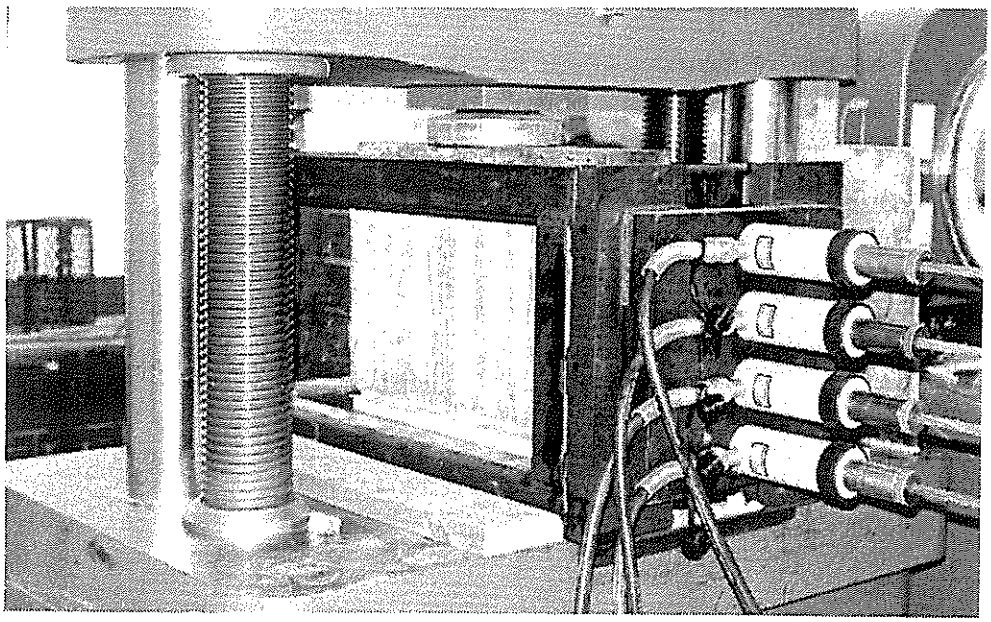

(b) Photograph of the biaxial test set-up

Figure 3
Set-up for biaxial test

Test Specimen

The specimen developed for purposes of biaxial testing is a rectangular slab as shown in Figure 4. In the center of the specimen is the test zone. Light reinforcement is placed in this zone in the form of a wire mesh to ensure a uniform stress transfer and a stable failure. The amount of reinforcement is small and does not affect the results. Tension is applied through reinforcing strands which are pulled by hydraulic jacks in the test set-up.

Compression is applied by means of the loading head block of the universal testing machine. Three steel plates (each 1 in thick) were used on both top and bottom surfaces, to develop a uniform state of stress. In addition, a teflon plate was placed on both surfaces of the specimen to eliminate frictional effects.

Seventy-four biaxial specimens were cast, cured and tested to obtain the response under biaxial stress conditions. Half these specimens were cured under controlled conditions in the laboratory and were tested after 28 days. The other half were cured under normal temperature and moisture conditions for 3 months before testing. Twelve standard ASTM beams, twelve cylinders for compressive strength, and six cylinders for split tensile test were also cast simultaneously to determine the uniaxial properties.

Additional biaxial tests were conducted on specimens of regular concrete patched with different shapes and depths of a repair material (shown in Figure 5). The patched specimens were cured under different conditions and for varying periods of time. Different ratios of biaxial stress, and predominantly tension-compression stresses, were applied to the patched regions to investigate the performance of the repair materials within rigid pavement slabs subjected to surface loading conditions. The patching depths were also varied to better represent the actual field conditions for the repaired pavements. Fifty specimens (similar to the one shown in Figure 5 with patching material) were tested in this phase of the study.

Standard ASTM load tests were carried out concurrently with the biaxial tests to assess the differences between the uniaxial and biaxial material response characteristics.

3.3 Uniaxial Tests on Biaxial Test Specimens

The specimens developed for biaxial tests were also tested in uniaxial stress states so as to obtain comparisons with standard tests. Uniaxial compression tests under monotonically increasing compressive stress were conducted for 21 specimens distributed over 4 groups of tests corresponding to non-patched and patched specimens at ages 28 days and 90 days. In addition, two different patch shapes (transition and rectangular) and three different patch depths of 2, 7 and 10 in were used. The compressive strengths obtained from these tests were less than those from standard tests. This is due to the effects of shape of specimen, size of specimens,

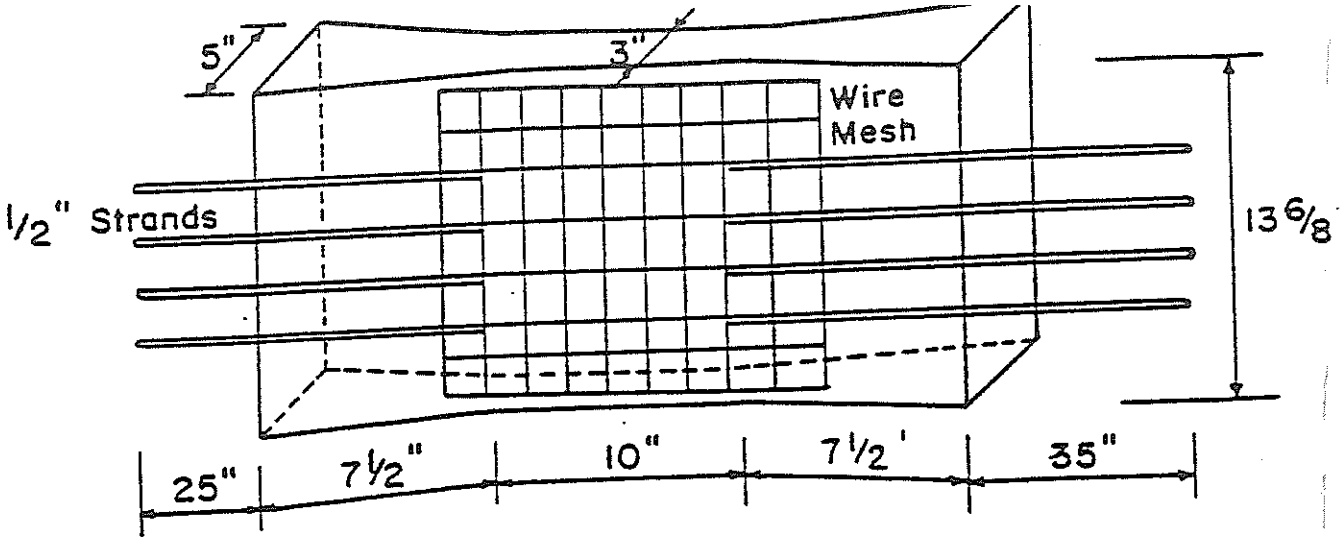

Figure 4
Details of the biaxial test specimen

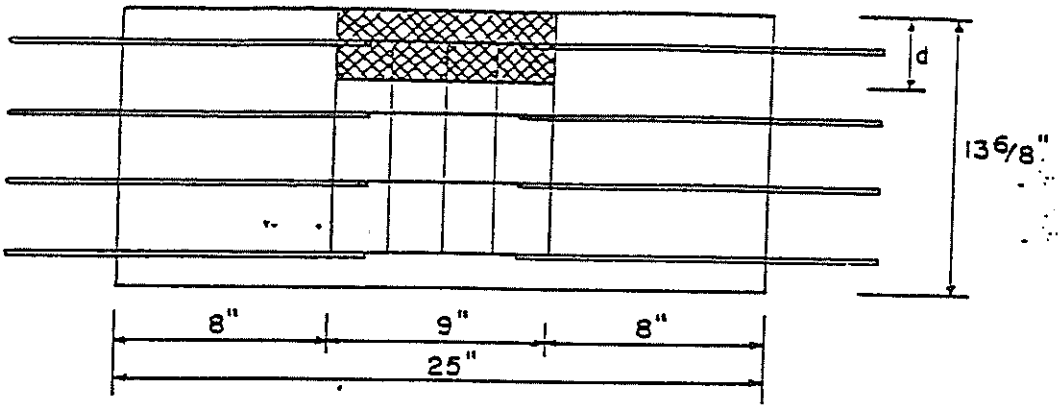

(a) Rectangular patch with various depth, d = 2, 7, and 10 in

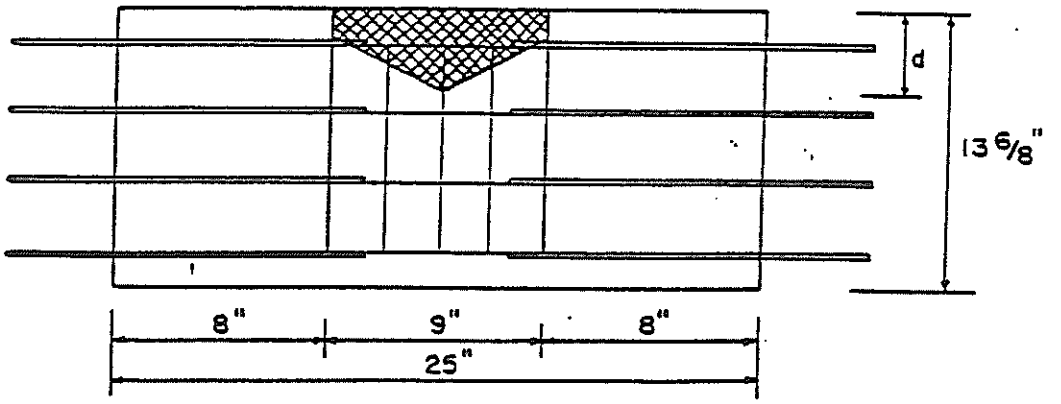

(b) Transition patch with d = 2, 7, and 10 in

Figure 5
Patch configuration in the biaxial test specimens

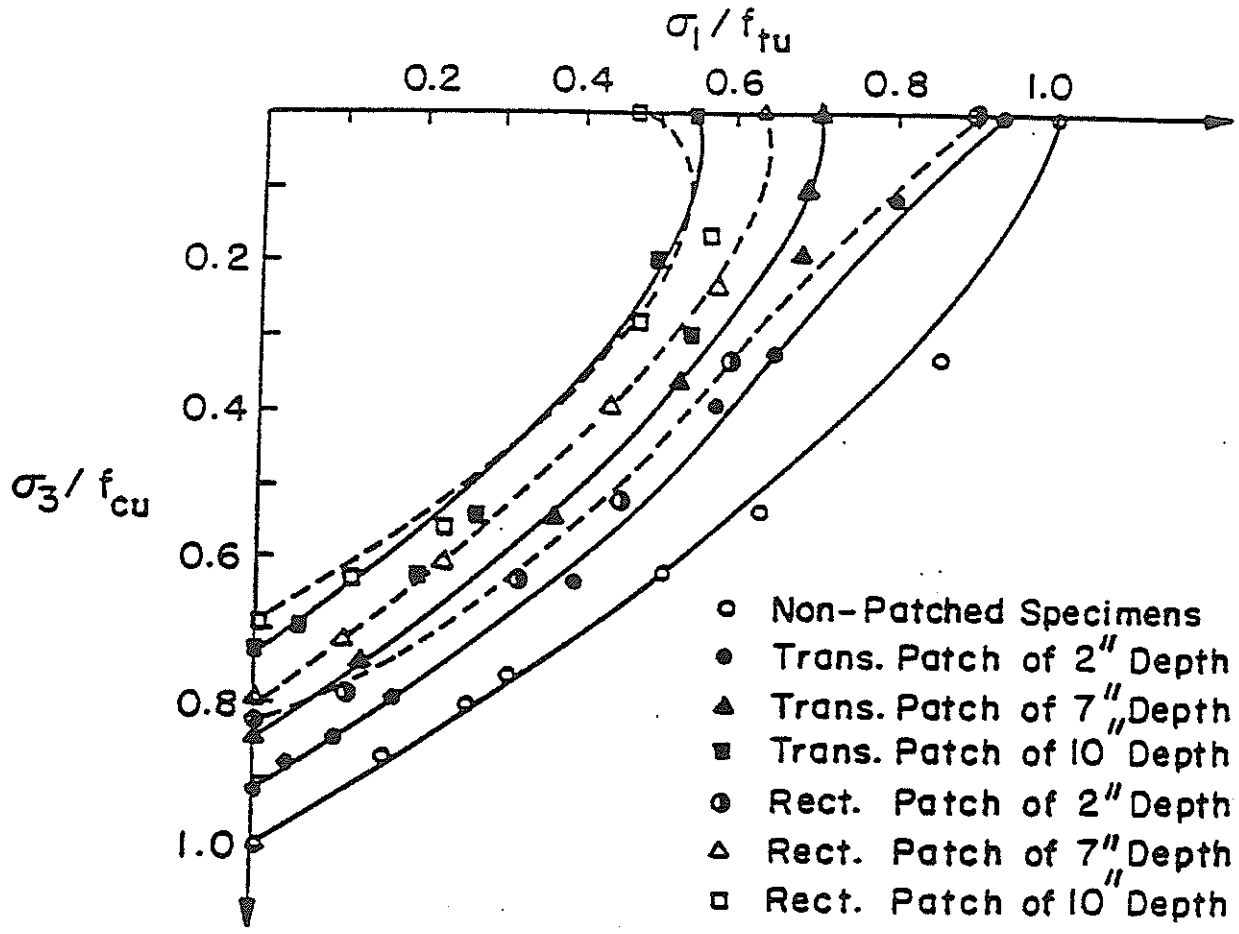

Figure 6
Ultimate strength envelope of patched specimens of age 28 days

4.2.2 Heating Patterns for Specific Cross Section Shapes

(1) For plates with strong axis bends, use vee heats as shown in Figure 3. Vee heats for any shape should follow the serpentine pattern shown in Figure 3.

(2) For Category S or W angles, use the vee and rectangular heat combination shown in Figure 4.

(3) For Category S or W wide flange beams, use the vee and rectangular heat combination shown in Figure 5.

(4) For Category S or W channels, use the vee and rectangular heat combination shown in Figure 6.

4.2.3 Plastic Rotation Computations for Plates and Rolled Shapes

The amount of plastic rotation removed per vee (or vee/rectangular) heat can be calculated from the following formula for various structural shapes. Multiple vee heats increase the plastic rotation in direct proportion as long as spacing between vees in greater than W.

$$\phi_p = F_t(T)\ F_L(M)\ F_s\ \varepsilon_p(T)\ \sin\frac{\theta}{3} \tag{9}$$

where F_t is the heating temperature factor ($F_t(T) = 0.5 + 0.0025\ (T-750)$ for all shapes), F_L is the restraining force factor, F_s is the shape factor, ε_p is the perfect confinement strain at the heating temperature, and θ is the vee angle.

For T = 1200°F and A36 steel

$$\phi_p = 0.0079\ F_L(M)\ F_s\ \sin\frac{\theta}{3} \tag{10}$$

(1) For plates with strong axis bends $F_s = 1$ and

$$F_L(M) = 0.9 + 3.4\ \frac{M}{M_p} \tag{11}$$

(2) For Category S or W angles

$$F_L(M) = (0.9 + 3.4\ \frac{M}{M_p})\ (1 + 2\ \frac{M}{M_p}) \tag{12}$$

$$F_s = 1 + \frac{1}{2}\ \frac{d_s b_s}{W^2} \tag{13}$$

(3) For Category S or W channels $F_L(M)$ is defined by Eq. 11, F_s is defined by Eq. 13 for Category S channels, and

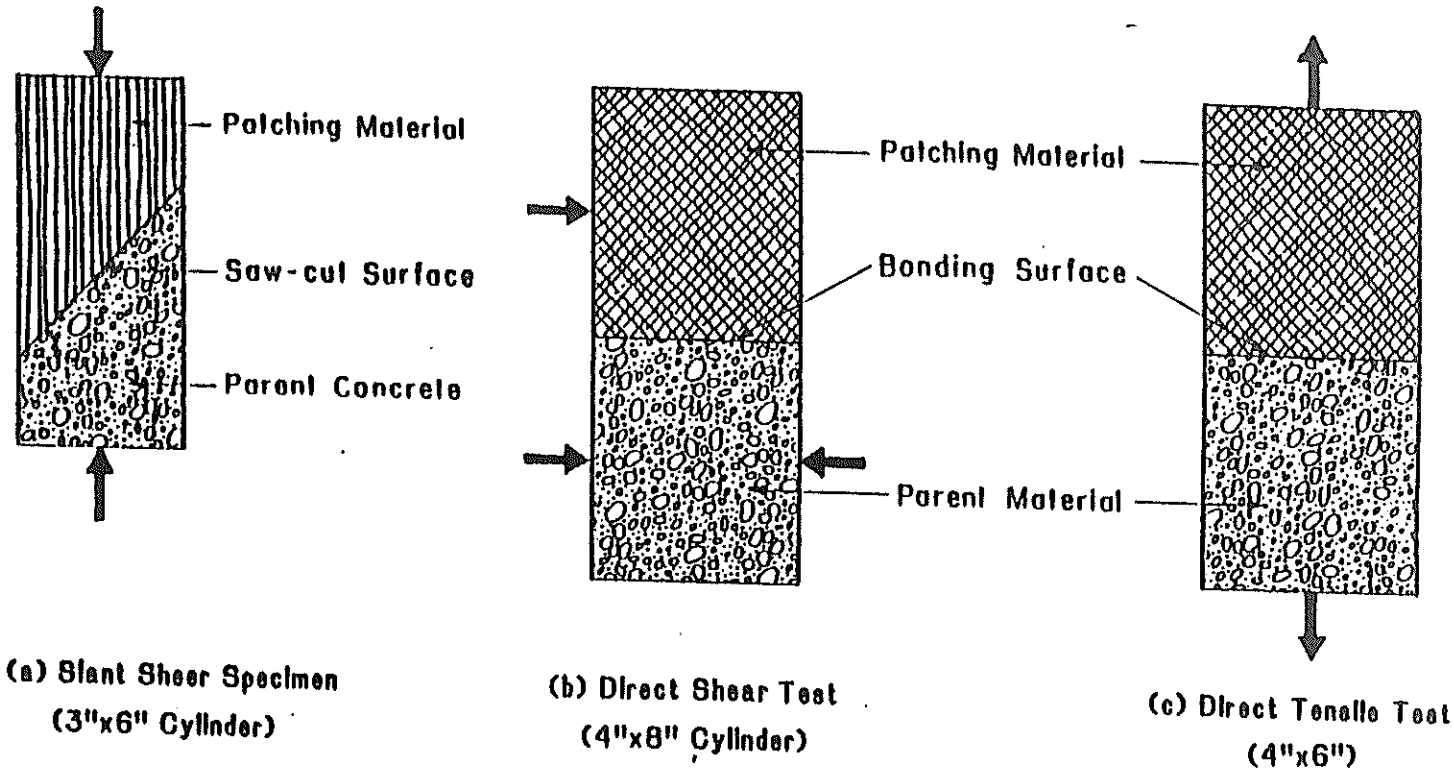

Figure 7
Laboratory bond strength tests

3.6 Shear Test of a Repaired Pavement Joint

In this phase of the experimental investigation, a number of repaired pavement joints were tested under transverse joint shear loading. Different patching configurations and depths (Figure 8) which are usually used in the field were studied. The repaired doweled joints were subjected to lateral loads, simulating the traffic axle loads, to investigate the performance of the repaired region under loading conditions similar to service conditions. These experiments determine the merits of a specific repair material and its bonding performance with the surrounding concrete in different repaired joints.

Tests were conducted on two different patch configurations (transition and rectangular) and three different patch depths (2, 4 and 6 in). Lateral loads simulating the effect of wheel loads were applied. There was no significant difference between the response of transition and rectangular patches. All the specimens tested failed by cracking, which started at the bottom of the specimen under the applied load and tended to change direction towards the interface between parent and patch material.

3.7 Steel Fiber Concrete

The content of the fibers for a given concrete depends primarily on the material properties that need to be improved and to what level. The upper limit of fiber content is dictated by the effect that the fiber has on the workability. On the other hand, the steel fiber content should not be below the lower limit, in order to get the acceptable benefit gained from the presence of the fiber. In the present work, 88 lb/yd^3 of XOREX steel fiber of 2 inch length and aspect ratio of 57 (length/diameter) was added to the concrete producing acceptable workability of the steel fibrous concrete. The volume of the fiber was 0.67 percent.

Aggregate shape and content are important factors that should be considered. The large aggregate size usually requires less fiber. Fine aggregate content for steel fiber concrete should be within the acceptable range (45-55 percent) of the total aggregate in order to produce a sufficient quantity of mortar in the concrete to separate the fibers and allow them to flow without tangling together. Cement factors are usually higher for steel fiber concrete than ordinary concrete. Typical cement factors range from 550 to 700 lb/yd^3 for 3/4 in aggregate. Cement content of 576 lb/yd^3 was used in the present work.

Addition of steel fibers was found to improve both flexural strength and toughness. The increase in toughness was more significant. This is expected to help in maintaining serviceability of pavements even after localized cracking occurs. In compression, addition of fibers was found to affect only the ductility. Failure in fiber concrete under uniaxial compression was preceded by the appearance of many inclined cracks.

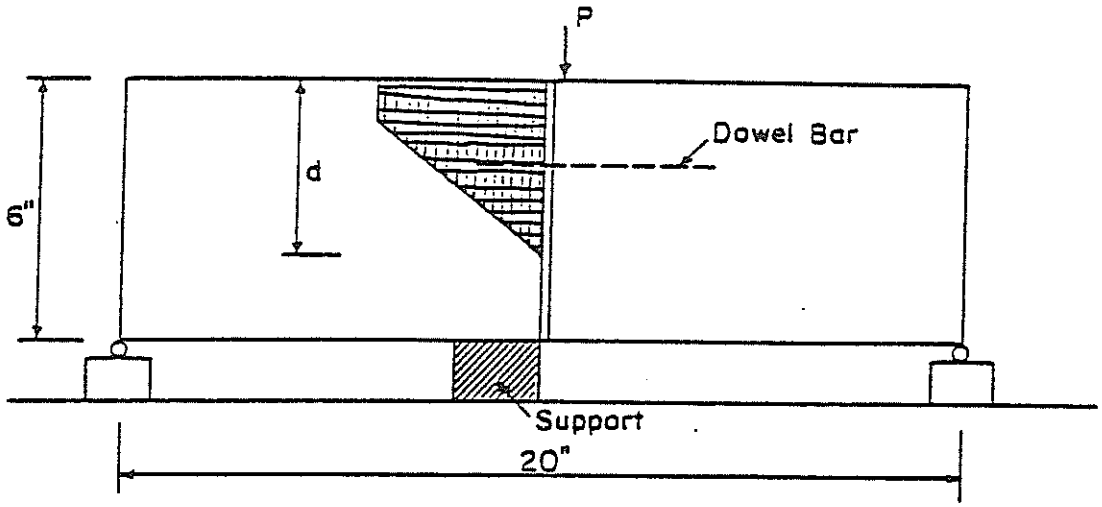

Figure 8a
Patch configurations in shear test of rigid joint (transition patch)

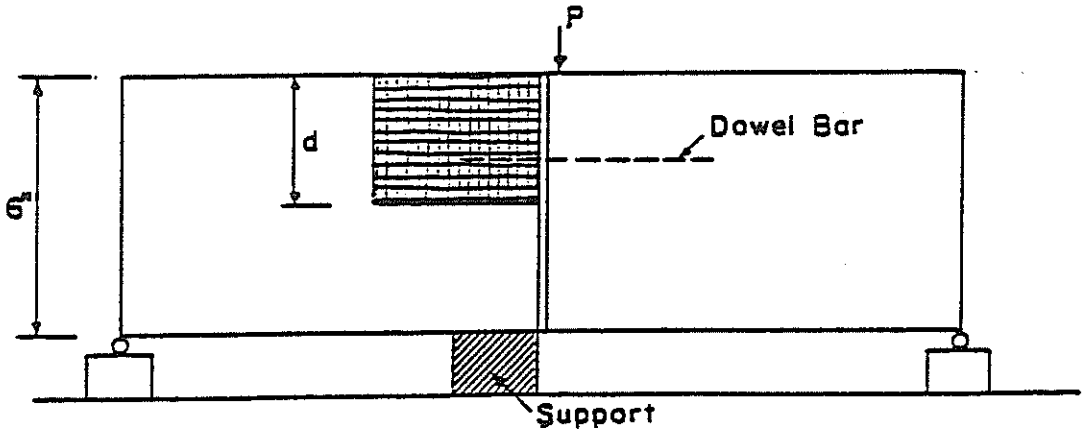

Figure 8b
Patch configurations in shear test of rigid joint (rectangular patch)

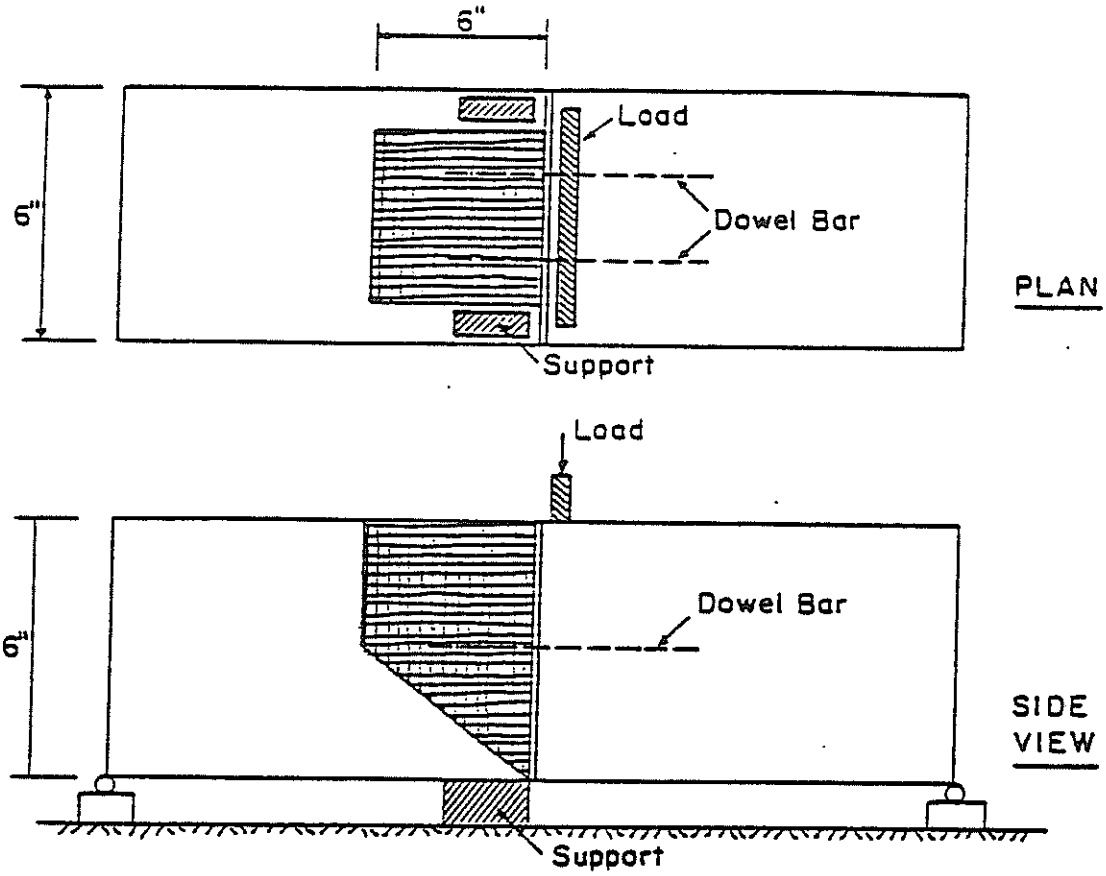

Figure 8c
Shear test of a repaired joint

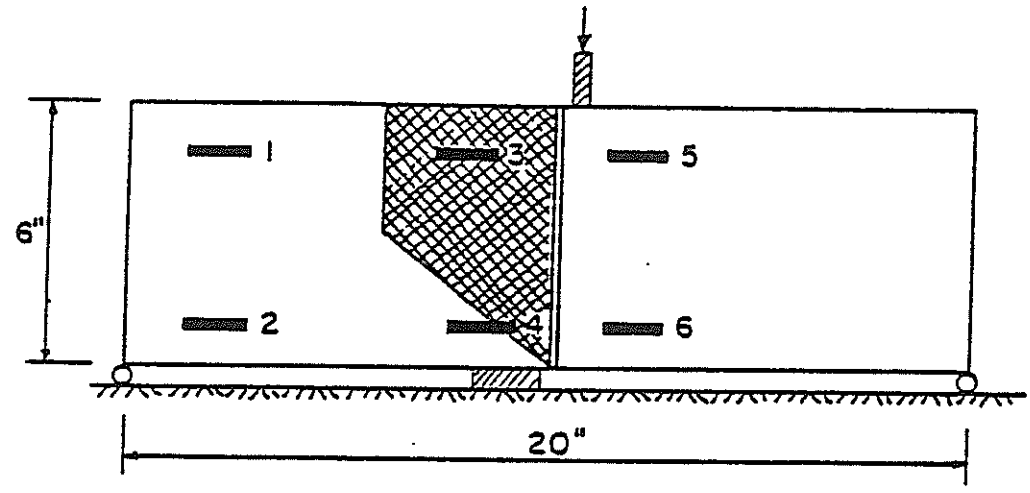

Figure 8d
Locations of the strain gages attached to a repaired joint specimen

Thirty specimens were cast, cured, and tested in biaxial tension-compression. Three groups of specimens, plain concrete, fiber reinforced concrete, and Duracal cement were prepared. Standard ASTM tests were also performed for comparison. In all three materials, the ultimate strength in tension under biaxial tension-compression stress states was found to be less than uniaxial tensile strength. The trend of response was the same for all three materials.

3.8 Rapid Patch Material (Duracal Cement)

Duracal cement contains Portland and gypsum cements which develop high, early strength, and expand slightly. It can be used neat or aggregated. In the present work, the proportion of Duracal cement to sand weight was 1:1 as recommended by the manufacturer.

A horizontal shaft mortar mixer was used in mixing the rapid patch material. Mixing was done by pouring in water and then adding one-half of the sand while the mixer was operating. Dry cement was then added to sand and water and finally the remaining sand was added. It was then mixed until it was lump-free, but not for more than five minutes. The mix was used immediately.

Unless a special test is specified, Duracal cement will set in approximately 20 to 45 minutes. It should be noted that dirty water and equipment will accelerate set of this material. Acceleration from dirty conditions, therefore, can cause problems.

Experimental specimens similar to the one shown in Figure 4 were cast, cured, and tested. The response of Duracal cement specimens was similar to that of plain concrete specimens.

3.9 Conclusions

An investigation was performed on the behavior of repair materials such as plain concrete, fiber concrete, and Duracal cement, as they respond in repaired regions of rigid pavements. Based on consideration of the test results described herein, the following conclusions concerning the behavior of brittle repair materials can be drawn.

1. The availability of a biaxial testing set-up for applying tensile and compressive loads simultaneously with a minimum of boundary conditions, and of accurate measurements, has been shown to provide better understanding by which the strength and behavior of brittle repair materials can be fully investigated. The test results presented show the capabilities of the biaxial tensile-compressive experimental technique.
2. Test results show that the strength of concrete under combined tension and compression is lower than the strength under uniaxial loading. The strength decrease is dependent on the principal stress ratio, i.e., the strength decreases as the applied tensile stress is increased.

3. For different biaxial stress ratios (σ_1/σ_3), the stress-strain curves possess the same general shape. However, both peak stress and corresponding strain decreased as the tensile stress (σ_1) increased.
4. For all uniaxial and biaxial tests, failure occurs by tensile splitting, with the fracture surface orthogonal to the direction of the maximum tensile strain.
5. Under combined tension and compression, a single continuous crack normal to the maximum tensile strain direction was formed except for ratios of the tensile stress to compressive stress smaller than 0.05 for which crushing fracture occurred.
6. Addition of steel fiber to concrete increases both flexural strength, peak tensile strain, and toughness. However, the increase in toughness was more significant and much higher than the increase in strength.
7. The addition of steel fiber to concrete had no effect up to the elastic limit of the tensile stress-strain behavior.
8. In uniaxial compression, the increase in strength due to the addition of steel fibers is insignificant. Duracal cement is stronger in compression in comparison with plain and fiber concrete.
9. Generally, fiber concrete possesses higher strength and ductility than plain concrete. However, the effect of adding fiber is different in the uniaxial state of stress than the biaxial tension-compression.
10. Duracal cement material has higher flexural strength and is more ductile than plain concrete but less than fiber concrete.
11. Plain concrete subjected to uniaxial compression and biaxial tension-compression failed by tensile splitting. Fiber concrete failed by faulting or shear failure.

Chapter 4

ANALYTICAL PROGRAM

4.1 Introduction

As already discussed, the simple test procedures can not suffice in identifying the critical factors for design and evaluation of repair configurations, materials, and procedures. In order to obtain additional information, a computer program was developed. This program can analyze both intact and patched concrete pavements considering different loading and support conditions, material properties, patch configurations, etc.

According to Majidzadeh *[2]*, any analytical program for modeling concrete pavements should be based on the finite element method, and should be capable of considering all the boundary, loading, and material characteristics expected in a pavement.

A review of available computer programs indicated that most of the programs employ plate elements for modeling the pavement. One of the main disadvantages of these models is their inability to consider the effect of the direct stress due to load and the stresses around the dowels. Particularly, concrete around the dowels is highly stressed, and local yielding, crushing, and cracking of concrete are encountered. These lead to a loss of dowel support after a number of repetitions of load, thus reducing the joint efficiency. Some researchers have employed commercial three-dimensional programs. These programs, besides being expensive, are available in compiled form only and hence, cannot be modified for specialized purposes, such as the simulation of cracking and other distresses in patched concrete pavements. Because of these considerations, a special purpose three-dimensional nonlinear finite element program was developed during the course of this study.

The program developed employs a special constitutive model for characterizing the response of concrete. The parameters required for using this constitutive model have hitherto been obtained from sophisticated testing techniques. In the experimental phase of this study, simple testing procedures, using available equipment, have been developed to obtain the necessary data. These procedures have been shown to be capable of reproducing the results obtained from more sophisticated tests.

The main objectives of this study are :

1. To develop a specialized finite element computer program for analyzing jointed concrete pavements.
2. To be capable of simulating jointed rigid pavement distresses due to loss of support, concrete deterioration due to fatigue, looseness of dowels, etc.

3. To be able to consider the development and propagation of cracks in pavements, and inelastic deformations of concrete.
4. To include the effects of night-time and day-time curling and warping of slabs.
5. To be able to analyze full and partial depth patched slab sections, and to study the effect of patching on the response, deflections, and stress levels in pavements.
6. To include the strains due to shrinkage in the analyses.
7. In this investigation, examples of full three-dimensional analyses of pavements and repair sections under combinations of self weight, wheel loads, and temperature are presented and discussed.

To be of real value to practicing engineers, the program will have to be used to analyze different pavement configurations on a case by case study and the results of such analyses could be employed fruitfully in arriving at alternative rehabilitation procedures.

In this study, for the first time, a complete distress simulation capability has been built into a three-dimensional analysis program and it is expected that analyses using this program would enable better understanding of pavement behavior, which can lead to proper guidelines for evaluation of different materials and repair procedures in rehabilitating rigid-jointed pavements.

4.2 Modeling of Concrete

In this study, concrete is modeled by means of three-dimensional quadratic finite elements. The material model employed considers both cracking of concrete and compressive yielding. This model was developed by Channakeshava and Iyengar *[3]* and is based on works of Rots, et al *[4]*. The model, along with an incremental, iterative analysis technique, can predict appearance and propagation of cracks, and yielding of concrete. Details are available in the full report *[5]*.

4.3 Modeling of Dowels and Dowel Support

Dowels are modelled through the beam elements. Thus, shear forces and moments in these bars can be considered. In order to simulate the interaction of dowels with the surrounding concrete, special dowel-concrete interface spring elements were developed. The stiffness of these springs can be found based on the condition of the joint. Provisions for dowel free-play can be made. A nonlinear stiffness variation can be chosen to realistically simulate the interaction between concrete and dowels.

4.4 Modeling of Subgrade

Two methods are available for modeling subgrade in a finite element analysis. The elastic foundation model, though more realistic, is computationally expensive. Also, difficulties are encountered in simulating loss of support during loading due to temperature curling effects, pavement uplift, etc. For these reasons, the simpler Winkler spring foundation model was employed in this study. In order to permit uplift of pavements, an iterative procedure was used to avoid tension in the subgrade springs. Local loss of support due to pumping was modelled by assuming a low stiffness for the corresponding subgrade springs.

4.5 Analysis Procedure

The procedure employed for the analysis is an incremental and iterative finite element procedure. As in any finite element procedure, the pavement is discretized using three-dimensional finite elements for concrete, beam elements for dowels, and spring elements for subgrade and dowel-concrete interface. Self weight loads and temperature strains are applied first and an analysis performed. Wheel loads are applied in small increments in the form of concentrated loads at prescribed nodes. For each increment of load, iterations are performed to obtain converged solutions considering cracking, yielding of concrete, and other nonlinearities. Failure is assumed when converged solutions could not be obtained within a prescribed maximum number of iterations. At the end of every increment, selected deflections and stresses are printed out.

4.6 Analysis of Jointed Concrete Pavements

4.6.1 Geometry and Materials

Any rehabilitation project should consider the mode of distress and its effect on the structural and functional performance of the pavements. An analytical study of simulated distress conditions helps in understanding these effects. The program developed in this study is applied to the analyses of typical pavement configurations under different loading conditions.

The pavement configuration employed for modeling concrete pavements is shown in Figure 9. Two adjacent slabs 20 ft x 12 ft x 0.833 ft each and a joint width of 0.025 ft. are considered. The dowels are of 1 inch diameter and 2 ft long, and are spaced at 1 ft. intervals. The subgrade is simulated through Winkler's spring model with a modulus of subgrade reaction of 691 kip/ft^3 (400 pci) corresponding to the cement stabilized base employed in Louisiana.

Three types of loading are considered for analysis. They correspond to the conditions of no temperature curling, night-time curling, and day-time curling respectively. In each load type, four support loss conditions, corresponding to: no loss,

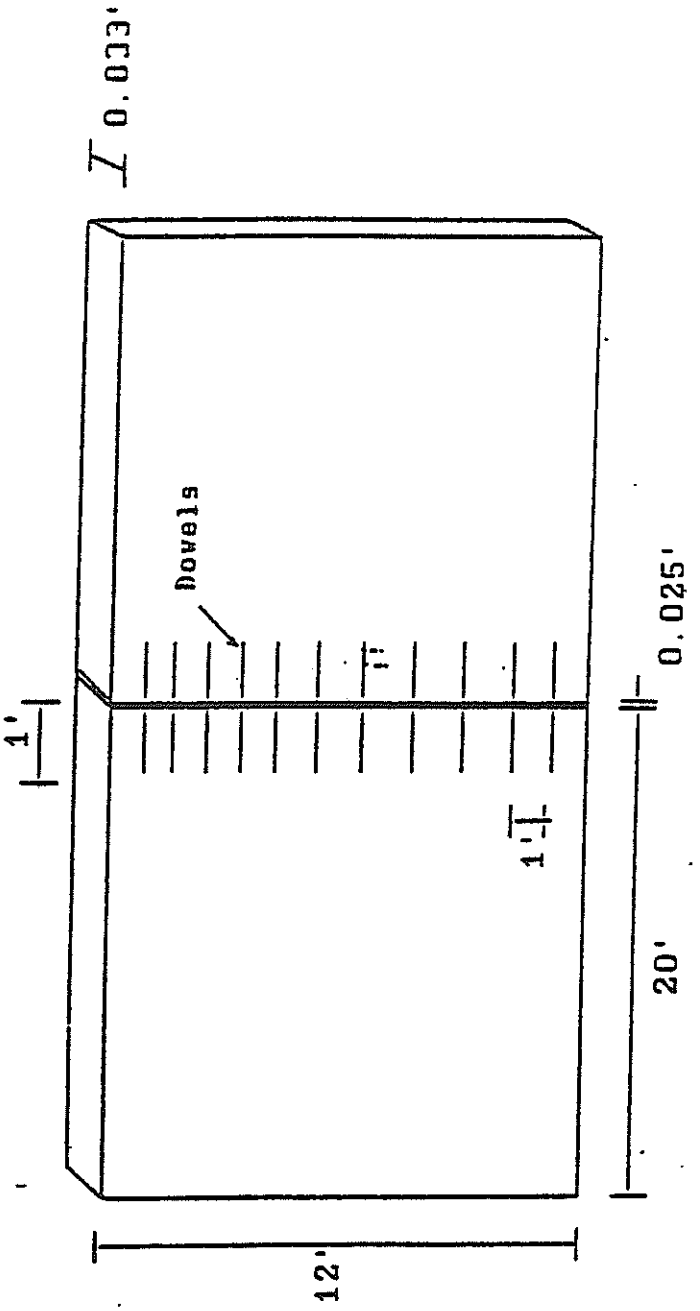

Figure 9
Selected pavement configuration

loss of support for 0.625 ft, 1.25 ft, and 4.375 ft, simulating different extent of loss due to pumping distress, are considered.

A detailed analysis of the joint region was performed to assess the effect of local yielding and cracking of concrete around dowels. This analysis resulted in the development of load-displacement response for the dowel-concrete interface springs. In analyzing pavements, both rigid dowel-concrete interface and a soft interface corresponding to the results of joint analysis were employed. Typical material properties were selected for concrete, dowels, and subgrade (Table 1).

4.6.2 Pavement under Self-Weight and Wheel Loads

The first case analyzed is that of a pavement subjected to self-weight and wheel loads corresponding to edge wheel path. In the first stage of the analysis only the self weight is applied as an increment of load. Subsequently, the wheel loads are applied in increments. The output at each increment consisted of maximum stresses, maximum displacements, and displacement at top surface along the edge wheel path. Four support conditions and two different dowel-concrete interface stiffness conditions were considered and eight analyses were performed.

Table 2 summarizes the result of the analyses. Figure 10 shows a typical deflected profile of the slabs. The vertical deflections are scaled 1000 times for purposes of plotting. Stress contours, possible crack pattern, and a comparison of deflection profiles for different cases is given in the main report *[5]*. One important observation was that if support loss is encountered under both slabs at the joint, the joint shear transfer efficiency, measured in terms of deflections of the two slabs, improves. This fact may prevent the detection of such voids, unless actual deflection values are considered.

4.6.3 Pavement under Self-Weight, Night-Time Temperature Gradient, and Wheel Loads

The second case analyzed is a pavement subjected to self weight, a temperature gradient corresponding to night-time curling (concave upwards) of 20°F at bottom and 0°F at top, and edge wheel loads. Table 3 summarizes the results of the analyses. Initially, only the self weight and the temperature gradients are applied. Then, wheel loads corresponding to edge wheel path are applied near the joint in increments and the solution continued. Figure 11 shows a typical deflection profile at an intermediate wheel load.

Stress contours and comparison of different deflection profiles can be found in the main report. It was observed that due to lift-off of the slabs at the joint during temperature curling, a partial loss of support resulted, which seemed to improve the shear transfer efficiency as explained earlier. For maximum support loss conditions, a rigid body rotation resulted and the far ends of the slabs were lifted up. Thus, faulting of slabs at a joint may also be due to loss of support at the other end of the slabs.

Table 1

Material properties for analysis of pavements

(A) Concrete

Young's modulus	: 761760.0 kips/ft^2 (36483 MPa)
Poisson's ratio	: 0.20
Density	: 0.145 kips/ft^3 (2.28 E-4 n/mm^3)
Compressive strength	: 576.0 kips/ft^2 (27.59 MPa)
Tensile strength	: 57.60 kips/ft^2 (27.59 MPa)
Fracture energy	: 0.01 kips/ft (0.146 kN/m)
Shear retention factor	: 0.2
Coefficient of thermal expansion	: 6.0E-6/deg.F

(B) Subgrade: (Note: Only compressive forces are resisted)

(I) For normal subgrade

Stiffness along x-axis (longitudinal)	: 1.0 kips/ft^3 (1.57 E-4 n/mm^3)
Stiffness along y-axis (transverse)	: 1.0 kips/ft^3 (1.57 E-4 n/mm^3)
Stiffness along z-axis (vertical)	: 691.0 kips/ft^3 (0.109 N/mm^3)

(II) For subgrade with loss of support

Stiffness along x-axis	: 1.0 kips/ft^3 (1.57 E-4) n/mm^3)
Stiffness along y-axis	: 1.0 kips/ft^3
Stiffness along z-axis	: 1.0 kips/ft^3

(C) Dowel-bars

Young's modulus	: 4291200.0 kips/ft^2 (205517 Mpa)
Modulus of rigidity	: 1650461.5 kips/ft^2 (79045 Mpa)
Area of cross section	: 0.00545414 ft^2 (506.7 mm^2)
Moment of inertia about y-axis	: 2.36785 E-06 ft^4 (20437 mm^4)
Moment of inertia about z-axis	: 2.36785 E-06 ft^4
Torsional moment of inertia	: 4.73573 E-06 ft^4 (40874 mm^4)

(D) Dowel-bar support springs

(I) For stiff springs

Stiffness along x-axis	: 1.0 kips/ft (14.6 N/mm)
Stiffness along y-axis	: 500,000 kips/ft (7.296 E+6 n/mm)
Stiffness along z-axis	: 500,000 kips/ft

Table 1 (continued)

(II) For soft springs

Stiffness coefficient along x-axis : 1.0
Stiffness coefficient along y-axis : 1.0
Stiffness coefficient along z-axis : 1.0

Load displacement curve :

Load		Displacement	
(kips)	(kN)	(ft)	(mm)
-4.50	-20.02	-8.66E-2	-26.40
-4.28	-19.04	-8.66E-4	- 0.264
-3.66	-16.28	-6.18E-4	- 1.884
-2.87	-12.77	-3.51E-4	- 1.01
-1.90	- 8.45	-1.22E-4	- 0.37
-1.05	- 4.67	-2.05E-5	- 0.062
1.05	4.67	2.05E-5	0.062
1.90	8.45	1.22E-4	0.37
2.87	12.77	3.51E-4	1.01
3.66	16.28	6.18E-4	1.884
4.28	19.04	8.66E-4	0.264
4.50	20.02	8.66E-2	26.40

Table 2

Summary of results of the analyses with load type 1

Support Condition	Dowel Support Conditions	Max. Load in Kips	Load @ Cracking in Kips	Compressive Stress in kips/ft^2			Maximum Deflection Due to Load in ft x 0.001		
				At 8 kips	At 20 kips	At Failure	Loaded	Unloaded	Efficiency (%)
1	Stiff	> 48	43	30.7	76.7	161.0 (42k)	1.80	1.73	95.3
	Soft	> 48	43	30.1	74.6	178.2	2.12	1.41	63.7
2	Stiff	44	36	30.5	76.4	168.0	2.90	2.82	97.0
	Soft	42	36	30.1	74.9	148.7	2.97	2.21	71.7
3	Stiff	32	26	31.1	77.7	124.2	4.13	4.05	97.6
	Soft	30	26	30.4	75.6	113.3	4.57	3.68	79.4
4	Stiff	12	10	52.2		68.8	11.05	11.01	99.5
	Soft	12	10	51.7		73.2	11.25	10.86	95.1

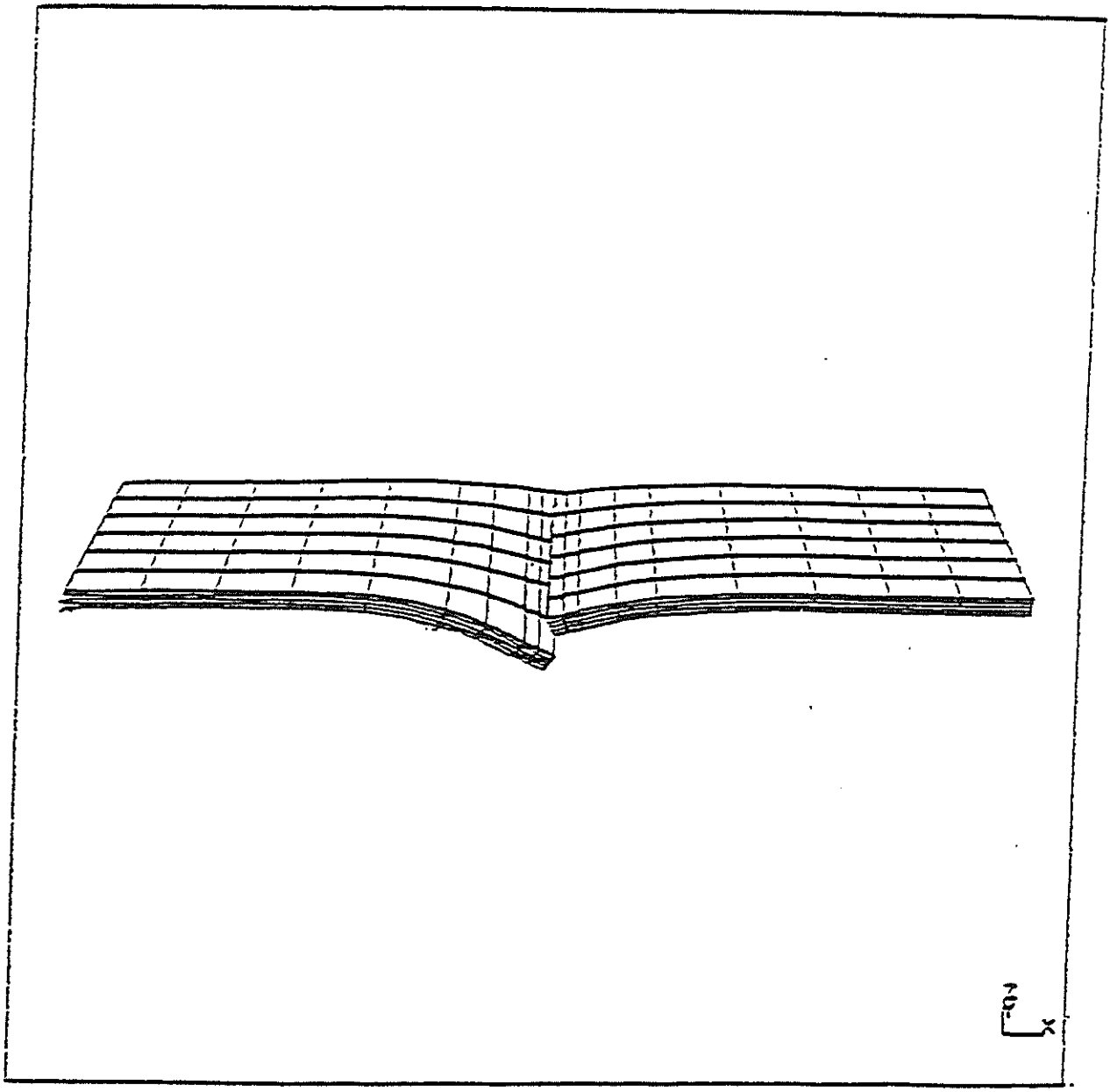

Figure 10
Typical deflected profile - load case 1

Table 3

Summary of results of the analyses with load type 2

Support Condition	Dowel Support Conditions	Max. Load in kips	Load @ Cracking in kips	Compressive Stress in kips/ft^2			Maximum Deflection due to Load in ft x 0.001		
				At 8 kips	At 20 kips	At Failure	Loaded	Unloaded	Efficiency (%)
1	Stiff	> 48	32	41.8	76.8	161.1 (42k)	4.65	4.57	98.3
	Soft	> 48	30	41.9	74.9	126.5 (34k)	5.01	4.24	84.7
2	Stiff	34	30	42.6	76.8	130.3	5.01	4.93	98.4
	Soft	32	26	42.5	75.1	119.8	5.25	4.58	87.2
3	Stiff	26	22	42.3	76.8	100.0	5.60	5.53	98.6
	Soft	24	20	42.4	75.3	90.5	5.94	5.20	87.5
4	Stiff	12	10	57.2		66.8	5.40	5.40	100
	Soft	12	9	57.1		67.2	5.44	5.43	99.8

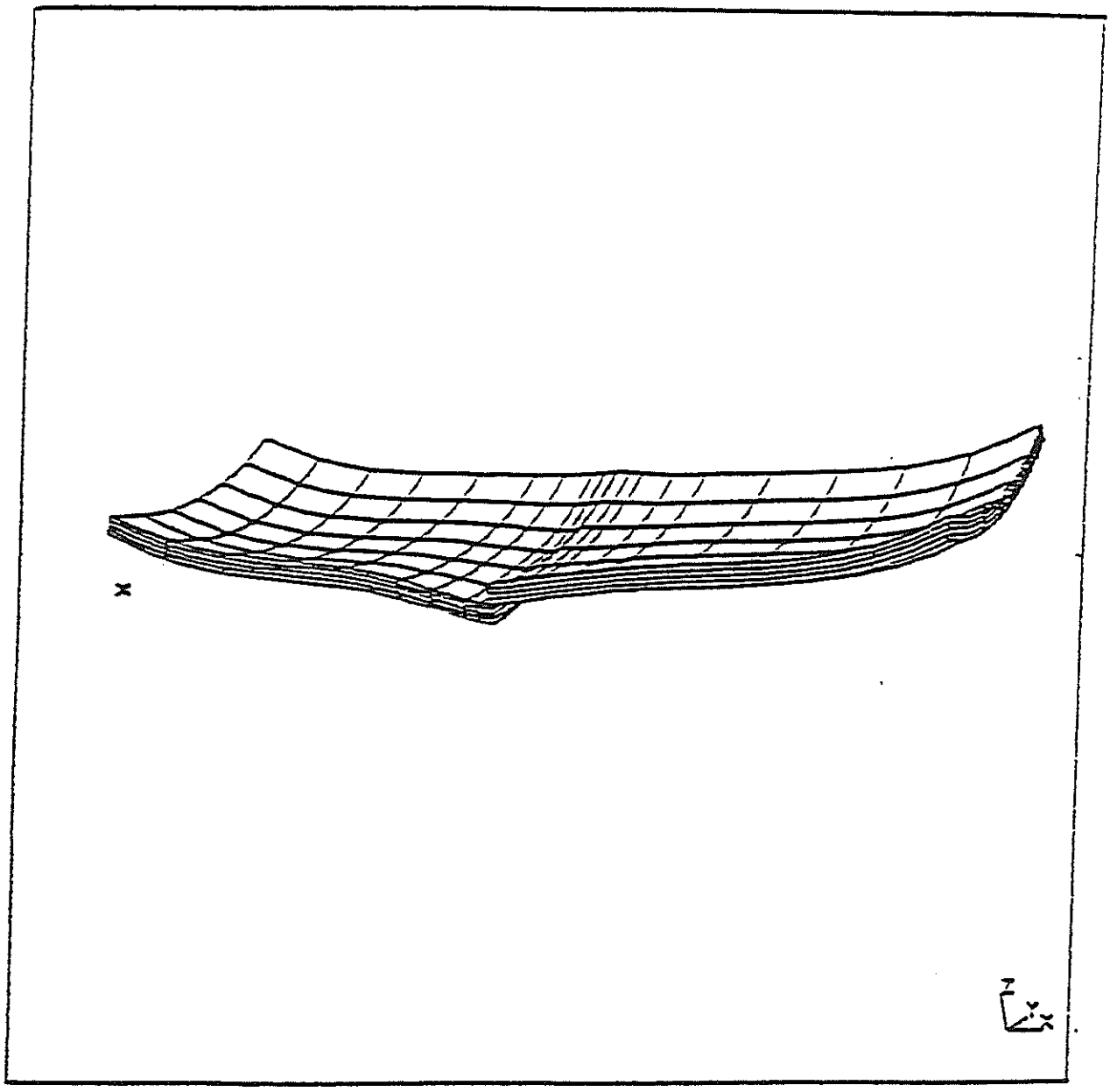

Figure 11
Deflection profile at an intermediate load - load case 2

4.6.4 Pavement under Self-Weight, Day-Time Temperature Gradient, and Wheel Loads

The third case analyzed is a pavement subjected to self weight, a temperature gradient corresponding to day-time curling (convex upwards) and edge wheel path loads. Again, the self weight and the temperature differential are applied first. Table 4 summarizes the results of the analyses. The deformed configuration under this load is shown in Figure 12. The behavior in this case is similar to that of no temperature gradient.

4.7 Study of Repaired Pavement Sections

4.7.1 Introduction

To develop an effective repair procedure, the mechanism of load transfer in a repaired pavement section should be well understood. Before embarking on repair work, the reasons of distress necessitating the repair should be evaluated and studied. The software developed in this study assists in such an investigative procedure. Next, the choice of a suitable repair material should be made based on an analytical study of the post-repair pavement section behavior. Repair works, being expensive, need much more investigative study than is currently made.

4.7.2 Effect of Shrinkage on Stresses in Repaired Pavements

In order to obtain information necessary for the evaluation of different repair materials, analyses are performed on full depth and partial depth patched concrete pavements. The material properties for the analyses are obtained from tests performed during the first part of this study. Two of the three repair materials, concrete and fiber concrete, are selected. The third material, used in the biaxial testing, Duracal cement, had properties very similar to concrete.

Shrinkage is an important parameter to be considered in the selection of a repair material. The existing concrete in the pavement has reached an equilibrium with the environment and not much volume change due to shrinkage or swelling can be expected in it. However, the new patch material undergoes considerable shrinkage during initial stages. Of the total shrinkage that this material undergoes, a part takes place while the material is still plastic. This does not generate any excess stresses. However, after some hardening takes place, further shrinkage occurs, which leads to stresses due to the restraints offered at the interface of the old and new materials. The effective shrinkage to be considered for the stress analysis is thus much less than the total shrinkage in the material. During the experimental phase of this project, shrinkage measurements were not made. Hence, in the analytical study, a parametric study was undertaken by varying the shrinkage strains in the patch material. Perfect bond was assumed at the interface of the old and new materials as no data regarding bonding properties was obtained during the tests.

Table 4

Summary of results for the analyses with load type 3

Support Condition	Dowel Support Conditions	Max. Load in kips	Load @ Cracking in kips	Compressive Stress in kips/ft^2			Maximum Deflection due to Load in ft		
				At 8 kips	At 20 kips	At Failure	Loaded	Unloaded	Efficiency (%)
1	Stiff	> 48	35	36.2	76.7	168.7 (44k)	1.81	1.73	95.8
	Soft	> 48	30	36.2	74.3	175.4	2.24	1.31	58.3
2	Stiff	44	36	33.2	76.4	170.3	2.64	2.56	97.1
	Soft	44	30	33.2	74.6	163.4	2.93	2.16	73.7
3	Stiff	34	28	31.1	77.3	131.3	4.16	4.08	98.1
	Soft	32	26	30.8	75.8	121.0	4.55	3.72	81.7
4	Stiff	12	9	53.3	--	70.8	9.64	9.58	99.4
	Soft	12	9	53.6	--	72.6	9.79	9.42	96.2

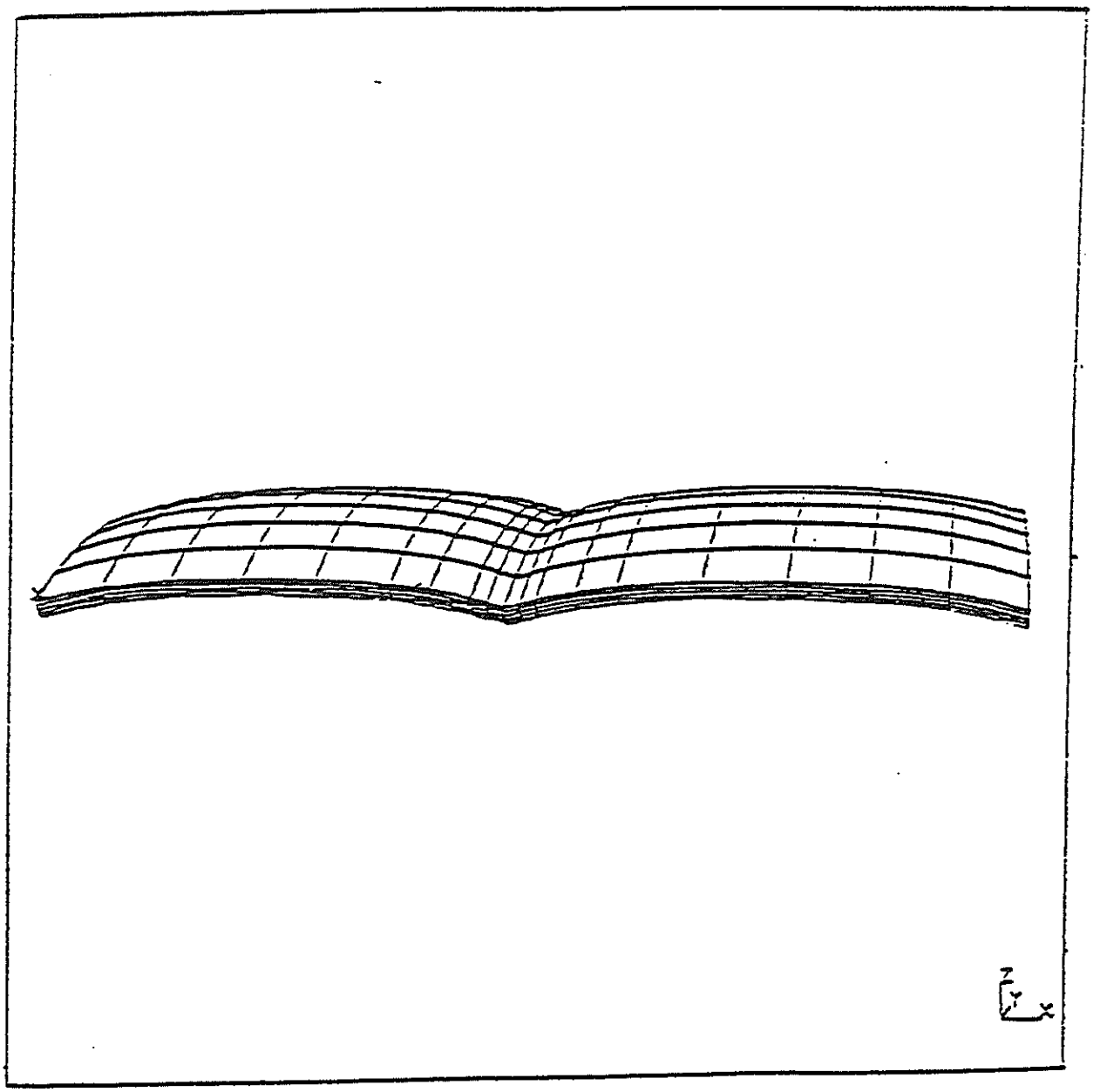

Figure 12
Initial deflection profile - load case 3

4.7.3 Analyses of Concrete Pavements with Full Depth Concrete Patches

Figure 13 shows the pavement layout selected for the analysis. The material properties employed for studying concrete-concrete full depth patched pavement are given in Table 5. One analysis was performed without any shrinkage strains and three more analyses were performed with shrinkage strains of 0.00003, 0.00005, and 0.00008. Dowel-concrete interface stiffness reflecting the local plasticity effects as described earlier is adopted. Two of the four cases were loaded to failure. Table 6 summarizes the results of the analyses.

At the interface between the two materials, while the existing material is subjected to compressive stresses, the repair material was subjected to tensile stresses. Also at the corner of the existing material, high tensile stresses developed. This aspect of the repair procedure needs particular attention since it is difficult to improve the existing material. Also, the existing material has exhausted a part of its fatigue life and there may be a corresponding loss of strength and stiffness. In these analyses, this loss is not considered.

Figure 14 shows the increase of maximum tensile stresses in the pavement with load for both the existing concrete and repair concrete for various shrinkage strains. It can be noted that, in case of analyses with shrinkage, considerable initial stresses are generated due to shrinkage. However, the difference in the stresses for the cases with and without shrinkage tends to reduce with load. For the existing concrete, high tensile stresses are generated only at the corners whereas the repair concrete is subjected to these high tensile stresses throughout the interface. Figure 15 shows a plot of the ratio of tensile stress to tensile strength with load. These curves are very useful for selecting the repair material. In cases where there is a likelihood of the occurrence of bi-axial compression-tension stress fields due to the combination of loads and support conditions, these curves reflect the effect of the strength reduction under such fields which have been observed experimentally. A special failure criterion employed in the program yields such a result. For different materials, some calibration may be necessary.

4.7.4 Analyses of Pavements with Full Depth Fiber-Concrete Patches

The material properties for studying the concrete-fiber concrete patched pavements are given in Table 7. As for the concrete-concrete patched pavements, four analyses with different shrinkage strains are performed. Table 8 summarizes the results of the analyses.

It was observed that the stresses due to shrinkage were higher for fiber concrete than for plain concrete patches. This is because of the higher difference in the modulus of elasticity between the existing and repair materials when fiber concrete is used as repair material. This implies that not only strength, but also the elastic

Table 5

Material properties for analysis of pavements with concrete patches

(A) Concrete

(I) Old concrete

Young's modulus	: 720000.0 kips/ft^2
Poisson's ratio	: 0.20
Density	: 0.145 kips/ft^3
Compressive strength	: 777.6 kips/ft^2
Tensile strength	: 55.0 kips/ft^2
Fracture energy	: 0.0132 kips/ft
Shear retension factor	: 0.05

(II) Patch concrete

Young's modulus	: 608342.0 kips/ft^2
Poisson's ratio	: 0.16
Density	: 0.145 kips/ft^3
Compressive strength	: 555.12 kips/ft^2
Tensile strength	: 53.0 kips/ft^2
Fracture energy	: 0.0132 kips/ft
Shear retension factor	: 0.05
Shrinkage strains	: 0.00003, 0.00005, 0.00008

(B) Subgrade

Note: only compressive forces are resisted

Stiffness along x-axis (longitudinal)	: 1.0 kips/ft^3
Stiffness along y-axis (transverse)	: 1.0 kips/ft^3
Stiffness along z-axis (vertical)	: 691.0 kips/ft^3

(C) Dowel-bars

Young's modulus	: 4291200.0 kips/ft^2
Modulus of rigidity	: 1650461.5 kips/ft^2
Area of cross section	: 0.00545414 ft^2
Moment of inertia about y-axis	: 2.36785 E-06 ft^4
Moment of inertia about z-axis	: 2.36785 E-06 ft^4
Torsional moment of inertia	: 4.73573 E-06 ft^4

Table 6

Summary of results of the analyses of pavements with full depth concrete-concrete patch

Shrinkage Level	Max. Load in kips	Load @ Cracking in kips	Material	Maximum Compressive Stress in kips/ft^2		Maximum Tensile Stress in kips/ft^2		Maximum Tensile stress to Tensile Strength ratio	
				Initial	@ 20 kips	Initial	@ 20 kips	Initial	@ 20 kips
1	> 33	22	Repair	0.69	63.64	0.73	49.06	0.01	0.89
			Existing	0.42	61.98	0.25	48.72	0.01	0.92
2	> 27	22	Repair	2.76	60.02	7.97	48.77	0.15	0.92
			Existing	8.35	64.56	6.59	54.08	0.12	0.98
3	> 27	18	Repair	6.90	57.94	19.87	50.55	0.38	0.95
			Existing	20.81	67.58	16.34	54.97	0.30	0.99
4	29	16	Repair	11.05	58.73	31.77	52.63	0.60	0.99
			Existing	33.30	72.56	26.09	54.41	0.47	0.99

Table 7

Material properties for analyses of pavements with fiber concrete patches

(A) Concrete

(I) Old concrete

Young's modulus	: 720000.0 kips/ft^2
Poisson's ratio	: 0.20
Density	: 0.145 kips/ft^3
Compressive strength	: 777.6 kips/ft^2
Tensile strength	: 55.0 kips/ft^2
Fracture energy	: 0.0132 kips/ft
Shear retension factor	: 0.05

(II) Patch fiber concrete

Young's modulus	: 936000.0 kips/ft^2
Poisson's ratio	: 0.16
Density	: 0.145 kips/ft^3
Compressive strength	: 603.5 kips/ft^2
Tensile strength	: 57.0 kips/ft^2
Fracture energy	: 0.33 kips/ft
Shear retension factor	: 0.05
Shrinkage strains	: 0.00003, 0.00005, 0.00008

(B) Subgrade

Note: Only compressive forces are resisted

Stiffness along x-axis (longitudinal)	: 1.0 kips/ft^3
Stiffness along y-axis (transverse)	: 1.0 kips/ft^3
Stiffness along z-axis (vertical)	: 691.0 kips/ft^3

(C) Dowel-bars

Young's modulus	: 4291200.0 kips/ft^2
Modulus of rigidity	: 1650461.5 kips/ft^2
Area of cross section	: 0.00545414 ft^2
Moment of inertia about y-axis	: 2.36785 E-06 ft^4
Moment of inertia about z-axis	: 2.36785 E-06 ft^4
Torsional moment of inertia	: 4.73573 E-06 ft^4

Table 8

Summary of results of the analyses of pavements with full depth fiber concrete-concrete patch

Shrinkage Level	Max. Load in kips	Load @ Cracking in kips	Material	Maximum Compressive Stress in kips/ft^2		Maximum Tensile Stress in kips/ft^2		Maximum Tensile stress to Tensile Strength ratio	
				Initial	@ 20 kips	Initial	@ 20 kips	Initial	@ 20 kips
1	46	22	Repair	0.46	64.40	0.27	50.92	0.01	0.89
			Existing	0.69	63.50	0.72	50.56	0.01	0.92
2	> 27	22	Repair	6.89	52.03	15.76	48.67	0.28	0.85
			Existing	14.26	66.14	9.86	54.55	0.18	0.99
3	> 27	18	Repair	11.49	63.18	26.25	50.54	0.46	0.89
			Existing	23.76	69.39	16.38	54.78	0.30	0.99
4	42	16	Repair	18.38	68.17	42.00	56.91	0.73	1.00
			Existing	38.00	76.36	26.16	54.95	0.48	1.00

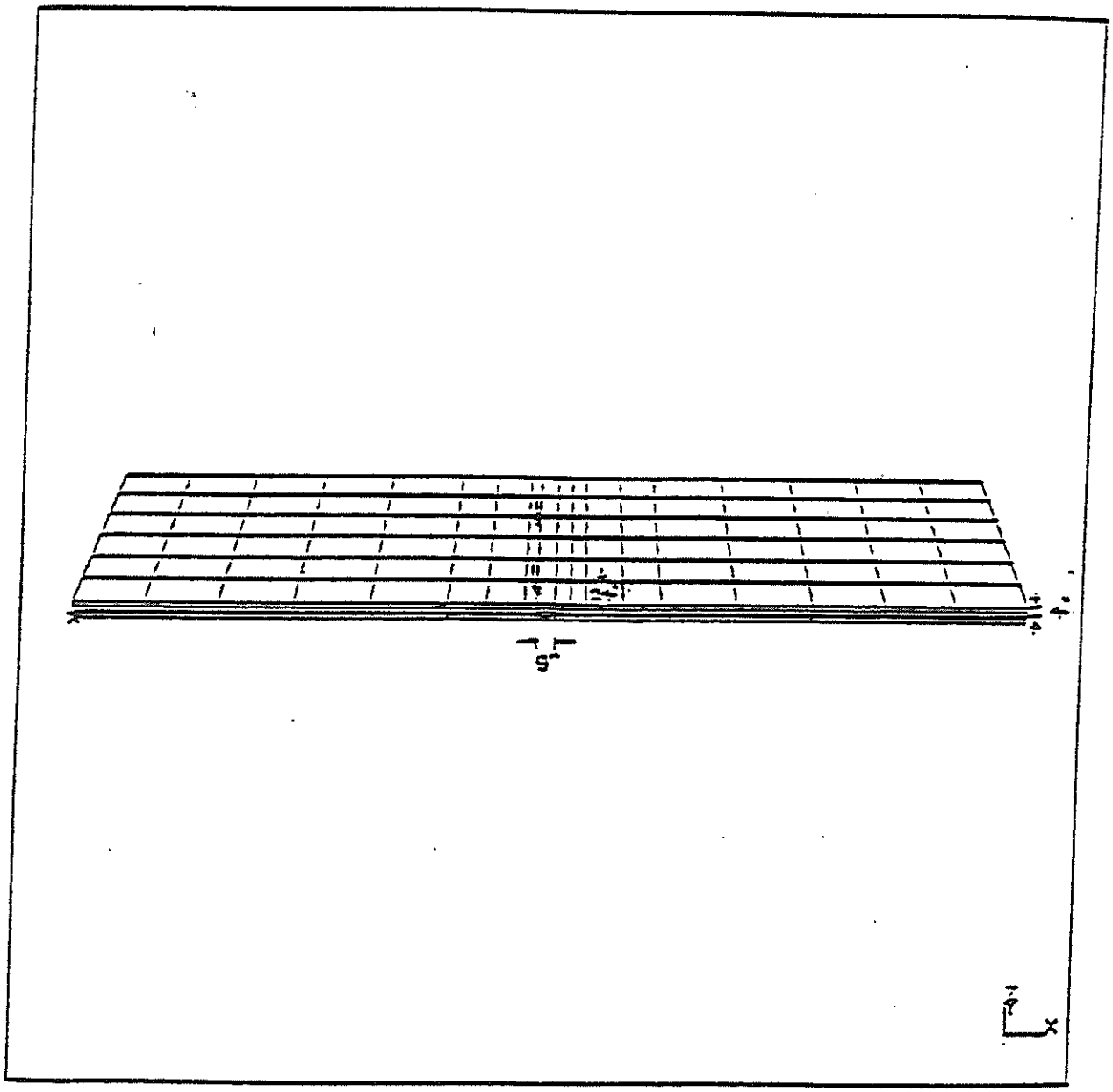

Figure 16
Partial depth patch configuration selected

Table 9

Summary of results of the analyses of pavements with partial depth concrete-concrete patch

Shrinkage Level	Max. Load in kips	Load @ Cracking in kips	Material	Maximum Compressive Stress in kips/ft^2		Maximum Tensile Stress in kips/ft^2		Maximum Tensile stress to Tensile Strength ratio	
				Initial	@ 20 kips	Initial	@ 20 kips	Initial	@ 20 kips
1	52	38	Repair	0.18	67.13	0.03	14.75	0.00	0.28
			Existing	0.54	83.37	0.48	28.78	0.01	0.52
2	> 27	--	Repair	5.05	65.82	12.18	20.66	0.23	0.39
			Existing	8.79	89.52	5.20	28.77	0.10	0.52
3	> 27	--	Repair	12.47	64.79	30.51	37.53	0.58	0.71
			Existing	21.73	99.12	13.01	32.06	0.24	0.58
4	46	28	Repair	19.93	64.97	48.84	51.73	0.92	0.98
			Existing	34.68	109.05	20.82	36.71	0.38	0.67

Table 10

Summary of results of the analyses of pavements with partial depth fiber concrete-concrete patch

Shrinkage Level	Max. Load in kips	Load @ Cracking in kips	Material	Maximum Compressive Stress in kips/ft^2		Maximum Tensile Stress in kips/ft^2.		Maximum Tensile stress to Tensile Strength ratio	
				Initial	@ 20 kips	Initial	@ 20 kips	Initial	@ 20 kips
1	52	38	Repair	0.22	74.45	0.05	16.00	0.00	0.28
			Existing	0.54	77.14	0.48	28.80	0.01	0.52
2	> 27	--	Repair	7.21	73.46	17.13	27.80	0.30	0.49
			Existing	10.99	84.76	6.89	28.79	0.13	0.52
3	> 27	--	Repair	17.98	73.73	42.88	51.00	0.75	0.90
			Existing	27.29	96.77	17.41	34.50	0.32	0.63
4	44	24	Repair	28.07	75.28	57.0	57.75	1.00	1.00
			Existing	43.34	108.80	23.63	40.55	0.43	0.74

shows the number of 9 kip ESAL in the same period of time. Now, the maximum permissible stress ratio for these two cases are given by the points S,T,U, and V corresponding to the two materials. These stress ratios can be used along with Figure 15 to determine the suitability of a selected material.

The following procedure can be employed for selecting a repair material. The additional information required for using this procedure is the maximum differential shrinkage strains that can be expected for the trial materials and their fatigue characteristics. These can be obtained from standard laboratory testing procedures.

1. Select the design life of the pavement after repairs. Corresponding to this design life, obtain the number of application of 18 kip ESALs from the traffic data for the pavement under consideration.
2. Select the trial patch material. From the fatigue curve for this material and for the existing material, obtain the permissible maximum stress ratios corresponding to the required ESAL applications computed in step 1.
3. From the curves in Figure 15, interpolate and obtain a curve corresponding to the effective shrinkage characteristics of the trial repair material.
4. From the given equivalent wheel load (for the 18 kip ESAL it is 9 kips), and from the interpolated shrinkage curve, obtain the maximum stress ratio. The maximum stress ratio thus obtained should be more than the permissible maximum stress ratio obtained in step 2. Apply this check for the existing material (note that the shrinkage curve is only for the repair material).
5. Steps 1 to 4 should be repeated for lower load levels, such as 9 kip ESAL.

If the criterion given in step 4 is satisfied for the different load levels, the trial material can be used for the repair work. If the criterion is violated, either a different material with better shrinkage characteristics should be tried, or special strengthening procedures such as reinforcing the interface or epoxy grouting can be adopted.

It should be noted that the curves obtained in Figure 15 are for a given value of Young's modulus of existing and patch materials, subgrade characteristics, and pavement geometry. Thus it may be necessary to reanalyze the pavements if significantly different values are to be used for the above properties.

Chapter 5

CONCLUSIONS

1. Local deformation of concrete around the dowels at the joints occurring due to high stress concentrations lead to a reduction in dowel concrete interface stiffness. In particular, with repetition of loads, the high stress levels developed lead to premature local failures. These failures, though highly localized, reduce the shear transfer efficiency of the joint.
2. The dowel-concrete interface stiffness has been found to affect the deflection profiles significantly under normal support conditions. This in turn affects the joint shear transfer efficiency which decreases with increase in load.
3. With loss of support under both slabs due to pumping damage, the shear transfer efficiency seems to increase even though the ultimate load reduces.
4. The corner load position due to edge wheel path leads to structural corner cracks. These cracks may appear even at service loads under severe loss of support conditions.
5. Night-time curling of slabs leads to a loss of support at the joints. It also widens the joint thus allowing entry of water at the joint. Most of the heavy traffic on highways travel in night and hence, night-time curling condition of the slab is more critical from a structural point of view.
6. The night-time curling of slabs, because of the loss of support under the joint, leads to a lift-off of the far end of the slab during the passage of heavy wheel loads. This effect is also present due to loss of support conditions due to pumping. Thus faulting of slabs at a joint may also indicate a loss of support at the far joint of that pavement slab.
7. Day-time curling condition is not critical to the joint. Further, the lift-off for this condition occurs at the center which is less frequently loaded. Another feature of this mode is that such a lift off does not encourage entry of water into the base of the slab. The behavior of pavements with day-time temperature gradients and wheel loads are similar to that due to no temperature gradients.
8. Shrinkage of repair materials is an important characteristic which affects the stresses in both repair and existing materials.
9. Due to shrinkage, corner cracks in the existing material at the junction of the repair and existing materials can be expected.
10. The increase in stresses increases with the difference in the Young's modulus of the existing and repair materials and with the maximum differential shrinkage for the two materials.

11. Shrinkage effects are significant only for low traffic loads. At higher traffic loads, the difference in maximum stresses for pavements with and without shrinkage stresses decreases.
12. Due to the increase in stress ratios at lower load levels, the fatigue life of the repaired section decreases.
13. Since the existing material is also affected by shrinkage of the patched material, selection of a very high quality repair material will not increase the life of the repaired section, unless the shrinkage difference between the two materials is small.
14. Partial patching procedures are more critical for material selection than full depth patching because of the additional interface between existing and repair materials. In addition, in these procedures, subgrade damage, if any, cannot be repaired. This also increases the stresses.

Chapter 6

RECOMMENDATIONS

The conclusions given above lead to the following recommendations:

1. Both the test procedure developed in this study for characterizing the repair materials, and the computer program which assists in selecting optimal patch configuration and repair material, should be used for developing an effective rehabilitation strategy.
2. Strength under biaxial tension-compression stress states should be investigated before selecting a repair material.
3. It is important to determine the elastic properties of the repair material in order to check for compatibility with the existing material.
4. Fiber concrete, with its higher post-failure energy dissipation capacity, is likely to maintain serviceability even after cracking.
5. Selection of pavement sections for rehabilitation should be done considering not only the damaged or faulted slab, but also the conditions at the far end of the adjoining slabs.
6. When measuring shear transfer efficiency to determine the extent of pumping damage, the actual deflections of the slab should also be considered. This is because loss of support under both slabs leads to an increase in shear transfer efficiency.
7. Shrinkage difference between the existing and patch material should be minimum for a satisfactory performance of the repair section. Failure of these sections can occur even in the existing material due to shrinkage.
8. The elastic properties of the repair material should be as close as possible to those of the existing material for reducing the shrinkage stresses.
9. Fatigue of existing and repair materials at low traffic loads should be investigated in the selection of rehabilitation procedure by estimating and including the shrinkage stresses.
10. In some cases, strengthening of the existing materials near the damaged region may be necessary for a satisfactory performance of the repair procedure.
11. The computer program developed in this study can be used as an effective tool in assessing the causes of distress of a concrete pavement and in selecting the optimal repair procedure and material.
12. The procedure described in the analytical part of this study may be employed during the selection of a repair material by considering both

fatigue and shrinkage. However, the fatigue characteristics need to be investigated and appropriately combined in the program.

REFERENCES

1. AASHTO Guide for Design of Pavement Structures, Publ. by the American Association of State Highway and Transportation Officials, 1986.
2. Majidzadeh, K., "A Mechanistic Approach to Rigid Pavement Design," in 'Concrete pavements', ed. by Stock, A. F., Elsevier Applied Science Publication, NY, 1988, pp. 11-56.
3. Channakeshava, C. and Iyengar, K. T. S., "Elasto-Plastic-Cracking Analysis of Reinforced Concrete," Journal of the Structural Division, ASCE, Vol. 114, No. ST11, November 1988, pp. 2421-2438.
4. Rots, J. G., Nauta, P., Kusters, G. M. A., and Blaauwendraad, J., "Smeared Crack Approach and Fracture Localization in Concrete," HERON, Vol. 30, No. 1, 1985.
5. Voyiadjis, G. Z, Channakeshava, C., Abu-Lebdeh, T. M., and Barzegar, F., "Engineering Properties of Brittle Repair Materials," Parts I and II, Final Report submitted to Louisiana Transportation Research Center, Baton Rouge, Louisiana, 1992.
6. Schrader, E. K., "Design Methods for Pavements with Special Concretes," Proceedings of International Symposium on "Fiber reinforced concrete", Ed. G. C. Hoff, ACI, SP 81-9, Detroit, 1984, pp. 197-212.